A Polyphenol-Rich Extract From Muscadine Grapes Inhibits Triple-Negative Breast Tumor Growth

Marianne Collard, PhD[1], Patricia E. Gallagher, PhD[1], and E. Ann Tallant, PhD[1] (iD)

Abstract

Triple-negative breast cancer (TNBC) is an aggressive subtype of breast cancer that tends to affect young women and has a high propensity to metastasize. No targeted treatments are available for this type of breast cancer due to a lack of estrogen or progesterone receptors or overexpression of human epidermal growth factor receptor type 2 overexpression. Currently, patients have no therapeutic options once standard of care is complete, indicating a need for safe and effective therapies to slow or prevent the progression of TNBC to metastatic disease. Studies showed that isolated polyphenols or polyphenol-rich muscadine grape extracts polyphenols inhibit the proliferation of various cancer cells including breast cancer. A proprietary muscadine grape extract (MGE) was administered to nude mice with human MDA-MB-231 TNBC atumors for 4 weeks to determine the effect of the extract on tumor growth. MGE decreased tumor volume in association with a reduction in the proliferative markers Ki67 and cyclin D1. To determine the molecular mechanisms for the MGE-induced reduction in tumor growth, mouse 4T1, MDA-MB-231, or human BT-549 TNBC cells were treated with MGE, and various signaling pathways were investigated. MGE reduced c-Met, differentially abrogated ERK/MAPK and AKT signaling, and decreased a downstream targets of ERK/MAPK and AKT pathways, cyclin D1. Cyclin D1 reduction was associated with retinoblastoma activation and cell cycle arrest in MDA-MB-231 TNBC cells. MGE-regulated molecular signaling pathways were functionally associated with a dose-dependent reduction in cell proliferation. The pluripotency of MGE and high index of safety and tolerability suggest that the extract may serve as a therapeutic to reduce TNBC progression to metastatic disease.

Introduction

Breast cancer will affect 1 in 8 US women in their lifetime.[1] Of these cases, 12% to 17% will be triple negative breast cancers (TNBC) that lack estrogen receptors or progesterone receptors and do not overexpress the human epidermal growth factor receptor (EGFR) type 2.[2] Due to this lack of receptor expression, there are currently no targeted treatments available for TNBC patients. Furthermore, TNBC is among the most aggressive subtypes of breast cancer.[3] Compared with other subtypes, the mean patient age is younger, the mean tumor size is larger, and patients are more likely to have invasive stage III tumors at the time of diagnosis. Patients with TNBC also have an increased mortality risk due to a lack of targeted treatment and a 4-fold increase in the likelihood of visceral metastases development within 5 years of diagnosis compared with other breast cancer subtypes.[4] Despite high initial response rates to

[1]Wake Forest School of Medicine, Winston-Salem, NC, USA

Corresponding Author:
E. Ann Tallant, Surgery/Hypertension & Vascular Research, Wake Forest School of Medicine, Biotech Place, 575 North Patterson Avenue, Suite 340, Winston-Salem, NC 27101, USA.
Email: atallant@wakehealth.edu

standard of care in TNBC, which includes surgery, radiation, and chemotherapy, recurrence is frequent, indicating that there are still cancer cells present after initial therapy.[5] Since these cells often progress to metastasis, which accounts for 90% of cancer-related deaths, an adjuvant therapy that inhibits proliferation of disseminated cancer cells would be a significant advancement in TNBC.[6]

Of interest are natural compounds with medicinal or health benefits, referred to as nutraceuticals, that have been used to treat and mitigate diseases since the advent of medicine. Nutraceuticals may be useful in cancer chemoprevention and treatment due to their pleiotropic mechanisms of action and low toxicity.[7] One extract studied as a cancer treatment is derived from muscadine grapes (*Vitis rotundifolia*).[8] Muscadine grapes are native to the Southeastern United States and are typically used to produce wine, juice, or jelly. Unlike other grapes, muscadine grapes contain low amounts of resveratrol and high amounts of ellagic acid.[9] Additional constituents found in muscadine grapes include gallic acid, quercetin, cyanidin, and delphinidin, which all individually exhibit anticancer activities.[10-12] Combinations of components such as these show enhanced antiproliferative activities compared with the individual components alone.[13-15]

The blend of active constituents in muscadine grapes and their enhanced synergistic activity show promise as a TNBC treatment. Luo et al[16] reported that an anthocyanidin- and ellagic acid–rich fraction of muscadine grapes induced cell cycle arrest and apoptosis in MDA-MB-231 TNBC cells. In other types of cancer, various muscadine grape extracts (MGEs) reduced proliferation of colon cancer cells by inducing apoptosis and altering cell cycle kinetics.[14] Hudson et al[15] demonstrated that a muscadine grape skin extract reduced the activation of multiple signaling pathways, including the AKT and extracellular-regulated kinase (ERK) mitogen-activated protein kinase (MAPK) signaling pathways, in prostate cancer cells. Further studies by this group showed that a muscadine grape skin extract induced G0/G1 cell cycle arrest in prostate cancer cells, which was associated with reduced cyclin D1 and increased p21.[17]

The reported effects of MGEs on proliferation and cell signaling suggest that an extract could be beneficial for the treatment of TNBC, which has a high proliferative index and overactive oncogenic signaling.[18] Both AKT and ERK1/2 phosphorylation lead to proliferation, survival, invasion, and angiogenesis.[19,20] ERK1/2 activation is involved in all steps of metastatic progression, and AKT activation ensures survival of cancer cells during and after metastatic colonization.[21] Due to their important role in metastasis, inhibiting AKT and ERK1/2 pathways to prevent TNBC metastatic progression is currently under investigation.[22] However, targeting the AKT or ERK1/2 signaling pathways individually has failed in clinical trials due to the highly heterogeneous and resilient nature of TNBC.[23] Current efforts are exploring effective combinatorial treatments that target multiple

signaling pathways.[24] In contrast, unfractionated natural products are inherently combination therapies since these agents contain numerous chemical compounds that may modulate different signaling pathways. The pleiotropic nature of a MGE thus may be effective for the treatment of TNBC. The present study investigated the anticancer potential of a proprietary MGE, composed of the polyphenol-rich seeds and skin, on TNBC cells and tumors.

Materials and Methods

Muscadine Grape Extract

A proprietary MGE powder derived from the seeds and skin of muscadine grapes from the Carlos variety was purchased from Piedmont Research and Development (Advance, NC). An aqueous extract was prepared, and the major components, measured by ultra-high-pressure liquid chromatography and mass spectroscopy, consisted of epicatechin, gallic acid, procyanidin B, ellagic acid, catechin, and catechin gallate; other phenolics including resveratrol were not detected.[25] All MGE concentrations are reported as the concentration of total phenolics quantified using the Folin-Ciocalteu method, with gallic acid as the standard.

Animal Model

The Wake Forest School of Medicine Animal Care and Use Committee approved the animal experiment. The fourth inguinal mammary fat pads of 6-week-old female athymic mice (Charles River, Wilmington, MA) were injected with 4×10^6 actively growing human MDA-MB-231 TNBC cells suspended in Matrigel (50:50). The mice were group housed in cages with HEPA-filtered air on 12-hour light/dark cycles and were fed standard mouse chow ad libitum. Tumor size was measured by caliper twice a week in conscious animals throughout the duration of the study. Administration of MGE was initiated when tumors were 100 mm^3 in size, determined using the equation for an ellipse $[(4/3)\pi r^3]/2$. The mice were randomized into either the control group receiving no treatment or the MGE group receiving 0.1 mg total phenolics/mL of MGE in their drinking water (corresponding to a dose of 0.5 mg total phenolics/mouse/day for a 25 g mouse). Four weeks after the intervention, the mice were sacrificed; the tumors were weighed and collected for analysis.

Immunohistochemistry

Tumors were fixed in 4% paraformaldehyde for 24 hours and immersed in 70% ethanol prior to paraffin embedding and sectioning at 5 μm. Staining for cyclin D1 (1:100; sc-20044 AF647; Santa Cruz, Dallas, TX) was performed using the Opal Multiplex IHC kit and fluorescent staining

protocol with 4′,6-diamidino-2-phenylindole (DAPI) as a counterstain (Perkin-Elmer, Waltham, MA). Staining for Ki67 (1:100; RM-9106-S; Thermo Fisher Scientific, Waltham, MA) was performed by the streptavidin-biotin method. Slides were deparaffinized in xylene, rehydrated through graded alcohols, and rinsed in water. Endogenous peroxidase activity was quenched by a 5-minute incubation in 3% peroxide. Antigen retrieval was performed in Dako Target Retrieval Solution (Agilent, Santa Clara, CA). Slides were then rinsed in phosphate-buffered saline (PBS), blocked with normal goat serum solution (NGS; 10% goat serum, 0.1 % bovine serum albumin, 0.1% Triton-X in PBS) for 30 minutes, blocked with Dako Serum-Free Protein block (Agilent) for 15 minutes and incubated overnight at 4°C with the primary antibody diluted in NGS. The following day, slides were washed in PBS, blocked with Dako Serum-Free Protein block for 10 minutes, and incubated with 1:400 biotinylated goat anti-rabbit antibody (Vector Laboratories, Burlingame, CA) in NGS for 1 hour. Slides were subsequently incubated with the avidin-biotin complex (Vector Laboratories) for 30 minutes, with 3,3′-diaminobenzidine (DAB) for 6 minutes and counterstained with Harris Hematoxylin (Newcomer Supply, Middleton, WI). Slides were dehydrated, cleared, and mounted with a coverslip. Negative controls with only the secondary antibody were performed to account for nonspecific binding. Cell positivity was determined using inForm software (Perkin-Elmer).

Cell Culture

4T1 (CRL-2539) Balb/cfC3H mouse stage IV breast cancer cells, MDA-MB-231 (HTB-26) human mammary adenocarcinoma cells and BT-549 (HTB-122) human ductal carcinoma cells were obtained from the American Tissue Culture Collection (Manassas, VA). All cell lines were authenticated by IDEXX BioAnalytics using short tandem repeat (STR) analysis, in November 2018 (Columbia, MO). 4T1 and BT-549 cells were grown in Gibco RPMI-1640 medium, and MDA-MB-231 cells were grown in Gibco Dulbecco's Modified Eagle Medium (Thermo Fisher Scientific). All media was supplemented with 100 μg/mL penicillin, 100 units/mL streptomycin, 15 mM HEPES, 2 mM L-glutamine, and 10% fetal bovine serum (FBS).

Transfection With Fluorescent Lentivirus

IncuCyte NucLight Red Lentivirus Reagent (EF1α, Puro) was purchased from Essen Bioscience (Ann Arbor, MI). A kill curve was performed for each cell line to determine the optimal concentration of puromycin used for antibiotic selection according to the protocol from Mirus Bio LLC (Madison, WI). Transfections were performed according to the manufacturer protocol. Briefly, cells were plated at 15% to 30% confluence and allowed to attach for 24 hours. The media was replaced with 100 μL of IncuCyte NucLight lentivirus reagent (MOI of 3) and 8 μg/mL polybrene in media (EMD Millipore, Darmstadt, Germany). Cells were incubated for 24 hours after which the transfection media was replaced with media containing the optimal dose of puromycin for the antibiotic selection. A maintenance concentration of 0.5 μg/mL puromycin was used in all subsequent passages to maintain a stable population of transfected cells.

Proliferation Assays

Cells were plated in a 96-well plate (Corning, NY) at densities of 4000 to 8000 cells/well depending on the cell type and incubated overnight in full-serum media. The next day, the media was replaced with 200 μL of 1% FBS media with the appropriate treatments. Proliferation was monitored with the IncuCyte ZOOM System (Essen BioScience), with images collected every 2 hours.

Western Blot

Cell lysates for western blot analyses were collected by solubilizing cells in Triton lysis buffer (100 mmol/L NaCl, 50 mmol/L NaF, 5 mmol/L EDTA, 1% Triton X-100, and 50 mmol/L Tris-HCl [pH 7.4]) containing 0.01 mmol/L $NaVO_4$, 0.1 mmol/L phenylmethylsulfonyl fluoride, and 0.6 μmol/L leupeptin and transferred into 1.5 mL Eppendorf tubes for storage at −20°C. The protein concentration of cell lysates was determined using the Bio-Rad Bradford protein assay (Hercules, CA) with bovine serum albumin as a standard. Western blots were performed using Bio-Rad reagents and equipment unless otherwise noted (Hercules, CA). Ten percent Mini-PROTEAN TGX Precast Protein Gels were loaded with 20 μg protein per well and transferred onto Immun-Blot PVDF (polyvinylidene difluoride) membranes. Primary antibodies were diluted in 5% bovine serum albumin or 5% Blotting-Grade Blocker in Tris-buffered saline with 0.1% Tween and applied to membranes overnight at 4°C with gentle agitation. Western blots were developed using SuperSignal West Femto Maximum Sensitivity Substrate (Thermo Fisher Scientific) and imaged using the ChemiDoc Touch Imaging System. Image Lab Software was used for analysis of immunoreactive bands, which were normalized to total protein/lane using a stain free gel.[26]

RNA Isolation/Quantitative Real-Time Polymerase Chain Reaction (qRT-PCR)

Cells were plated at 25% confluency in 10% FBS. The following day, the media was changed to 1% FBS media and incubated for 24 hours, at which time 20 μg total phenolics/mL of MGE was added to the cells. After either 1 hour, 6 hours, 12 hours, or 24 hours of treatment, RNA was isolated using the Trizol reagent according to the manufacturer's

protocol (Thermo Fisher Scientific). RNA concentration and integrity were assessed with an Agilent 2100 Bioanalyzer with an RNA 6000 Nano LabChip (Agilent Technologies, Palo Alto, CA). Total RNA (1 µg) was reverse transcribed; the resultant cDNA (2 µL) was added to TaqMan Universal PCR Master Mix (Applied Biosystems, Foster City, CA) with gene-specific primer/probe sets; amplification was performed on the ABI QuantStudio 3 Detection System. All reactions were performed in triplicate; 18S ribosomal RNA amplified using the TaqMan rRNA control kit (Applied Biosystems) served as an internal control. Results were quantified as cycle threshold (Ct) values, where Ct is the threshold cycle of PCR at which amplified product is first detected, and expressed as the ratio of target/control (Relative Gene Expression) using the $2^{-\Delta\Delta Ct}$ method.

Cell Cycle Analysis

Cells were plated at 50% confluence in 60-mm dishes in full-serum media. The next day, cells were serum starved for 24 hours, and then the media was changed to 1% FBS media with respective treatments for 24 hours. Media and trypsinized cells were collected, pelleted by centrifugation, fixed in 66% ethanol, and stored at 4°C. Before analysis by flow cytometry, cells were stained with propidium iodide (ab139418) according to the manufacturer's protocol (Abcam, Cambridge, UK). Flow cytometry was performed using the BD FACSCalibur, and data were acquired using FCS Express 6 DNA cell cycle analysis program (BD Biosciences, San Jose, CA; De Novo Software, Los Angeles, CA).

Apoptosis Assay

Cells were seeded in 10% FBS media overnight at a density of 4000 cells/well in a 96-well plate. The next day, MGE at the concentrations indicated was added to the cells in 1% FBS media containing 5 µM of the IncuCyte Caspase-3/7 Apoptosis Reagent (Essen BioScience Cat #4440). Staurosporine was used as a positive control for apoptosis. Images were collected every 2 hours after treatment using the IncuCyte ZOOM System (Essen BioScience), and caspase 3/7 activation was monitored by green fluorescent staining of nuclear DNA.

Reagents (Antibodies and Primers)

The antibodies used in this study were as follows: c-Met (1:1000, #8198 with human reactivity only; 1:1000, #3127), c-Raf (1:500, #9422), pp44/42 MAPK (pERK1/2, 1:1000, #4376), p44/42 MAPK (ERK1/2, 1:1000, #9102), pMEK1/2 (1:1000, #9154), MEK1/2 (1:1000, #9122), pAKT (Ser473, 1:2000, #4060), AKT (1:1000, #9272), cyclin D1 (1:1000,

#2922), pRb (Ser780, 1:1000, #8180) were obtained from Cell Signaling (Danvers, MA) and Anti-Rb (1:1000, ab24) from Abcam. Antibody verification information is provided in Table 1. TaqMan gene expression assay (FAM) inventoried gene-specific primer/probes (#4331182) were used for qRT-PCR (Thermo Fisher Scientific).

Statistical Analysis

Statistical analysis was performed by 1-way analysis of variance using the GraphPad Prism 6 software. Results were considered significant when $P < .05$. All data are presented as mean ± SEM.

Results

MGE Inhibits Tumor Growth and Oncogenic Signaling In Vivo

In pilot studies, mice were treated with increasing concentrations of MGE (from 0.01 to 0.2 mg total phenolics/mL of MGE), and toxicity and inhibition of tumor growth were measured to determine a nontoxic concentration of MGE with maximal tumor growth (data not shown). Athymic mice with MDA-MB-231 (human) tumors in their mammary fat pads were subsequently treated for 4 weeks with 0.1 mg total phenolics/mL of MGE (Figure 1A). MGE significantly reduced tumor size from 1304 ± 96 mm³ in untreated mice to 631.5 ± 82 mm³ in MGE-treated mice (Figure 1B). Immunohistochemical analysis of tumors showed that MGE significantly reduced cyclin D1 from 0.81 ± 0.28% positive cells in control mice to 0.20 ± 0.05% positive cells in MGE-treated mice (Figure 1C and D) and Ki67 from 10.9 ± 0.98% in control mice to 7.34 ± 0.37% in MGE-treated mice (Figure 1E). These results indicate that MGE inhibits tumor growth in association with a reduction in cyclin D1 and E2F target protein Ki67.

MGE Inhibits Proliferation of TNBC Cells

In order to identify the molecular mechanisms for the growth inhibitory effects of MGE, the effect of MGE on cell proliferation *in vitro* was determined using 4T1 (murine), MDA-MB-231, and BT-549 (human) TNBC cells treated with increasing concentrations of MGE. MGE inhibited the proliferation of all cell lines in a time- and dose- dependent manner at concentrations of 5 µg total phenolics/mL to 25 µg total phenolics/mL (Figure 2A-C). After 48 hours of treatment, 20 µg total phenolics/mL of MGE inhibited proliferation of 4T1 cells by 88.7% (6.2 ± 0.3 vs 0.7 ± 0.1, nuclei red count fold change from time 0 hour), MDA-MB-231 cells by 44.4% (2.7 ± 0.18 vs 1.5 ± 0.03), and BT-549 cells by 25.0% (1.6 ± 0.05 vs 1.2 ± 0.07). Representative images for each cell line show the reduction in cells, denoted by red

Table 1. Antibody Verification. Antibodies Used in This Study Are Displayed in the Left Column With Corresponding Links to Antibody Verification in the Right Column.

Antibody	Proof of Verification
c-Met (#8198) Cell Signaling	https://www.antibodypedia.com/gene/3939/MET/antibody/167049/8198
c-Met (#3127) Cell Signaling	https://www.antibodypedia.com/gene/3939/MET/antibody/106296/3127
c-Raf (#9422) Cell Signaling	https://www.antibodypedia.com/gene/1131/RAF1/antibody/107963/9422
Phospho-p44/42MAPK (pERK1/2) (#4376) Cell Signaling	https://app.benchsci.com/product/Cell%20Signaling%20Technology/4376/figures
p44/42 MAPK (ERK1/2) (#9102) Cell Signaling	https://app.benchsci.com/product/Cell%20Signaling%20Technology/9102/figures
Phospho-MEK1/2 (#9154) Cell Signaling	https://app.benchsci.com/product/Cell%20Signaling%20Technology/9154/figures
Phospho-AKT (Ser473) (#4060) Cell Signaling	https://www.antibodypedia.com/gene/135/AKT1/antibody/106995/4060
AKT (#9272) Cell Signaling	https://www.antibodypedia.com/gene/135/AKT1/antibody/166716/9272
Cyclin D1 (#2922) Cell Signaling	https://www.antibodypedia.com/gene/3660/CCND1/antibody/106168/2922
Phospho-Rb (Ser780) (#8180) Cell Signaling	https://app.benchsci.com/product/Cell%20Signaling%20Technology/8180/figures
Anti-RB (ab24) Abcam	https://app.benchsci.com/product/Abcam/AB24/figures
Cyclin D1 (DCS-6) (sc-20044) Santa Cruz	https://app.benchsci.com/product/Santa%20Cruz%20Biotechnology/SC-20044/figures
Ki67 (SP6) (RM-9106-S1) Thermo Fischer	https://app.benchsci.com/product/LabVision/RM-9106-S1/figures

fluorescent nuclei, after 24 hours of treatment with 20 μ total phenolics/mL of MGE compared with the untreated control cells (Figure 2A-C). These results demonstrate that MGE inhibits TNBC proliferation in both a time- and dose-dependent manner. Contrary to other MGE extracts previously studied, the proprietary MGE did not induce apoptosis in any of the TNBC cell lines, suggesting that MGE is reducing proliferation independent of apoptosis[15,16] (Supplemental Figure 1, available online).

MGE Inhibits c-Met Protein in TNBC Cells

c-Met, also known as hepatocyte growth factor receptor (HGFR), is a receptor tyrosine kinase that stimulates cell cycle progression, survival, motility, invasion, and proliferation through AKT and MAPK/ERK signaling.[27] Both c-Met total protein and *MET* mRNA were significantly reduced with MGE treatment in all cell lines as determined by western blot analysis and qRT-PCR (Figure 3). c-Met protein was reduced by 51.4%, 99.8%, and 40.8% in 4T1, MDA-MB-231, and BT-549 cells treated with 20 μg total phenolics/mL of MGE, respectively (Figure 3A-C). Representative western blots are depicted below the graphs and show decreased band intensity with MGE treatment.

c-Met protein was almost absent in MDA-MB-231 cells after treatment with both doses of MGE for 36 hours. After 24 hours of treatment with 20 μg total phenolics/mL of MGE, *MET* mRNA was reduced by 57.5%, 36.4%, and 57.4% in 4T1, MDA-MB-231, and BT-549 cells, respectively (Figure 3D-F). These results suggest that MGE reduces the amount of the c-Met receptor in TNBC cells through transcriptional regulation of *MET* or by destabilizing the mRNA transcripts.

MGE Inhibits Proliferative Signaling in TNBC Cells

The AKT signaling pathway is downstream of c-Met and regulates cell proliferation and survival.[28] Treatment of 4T1 and BT-549 cells with 20 μg total phenolics/mL of MGE reduced AKT activation at serine 473 by 52.7% and 30.4%, respectively (Figure 3G and I). In MDA-MB-231 cells, both 10 μg total phenolics/mL and 20 μg total phenolics/mL of MGE inhibited phosphorylation of AKT by over 64% (Figure 3H). Representative western blots of phospho-AKT and respective total AKT protein are shown below the graphs. The lower dose of MGE did not inhibit AKT phosphorylation in 4T1 and BT-549 cells, suggesting
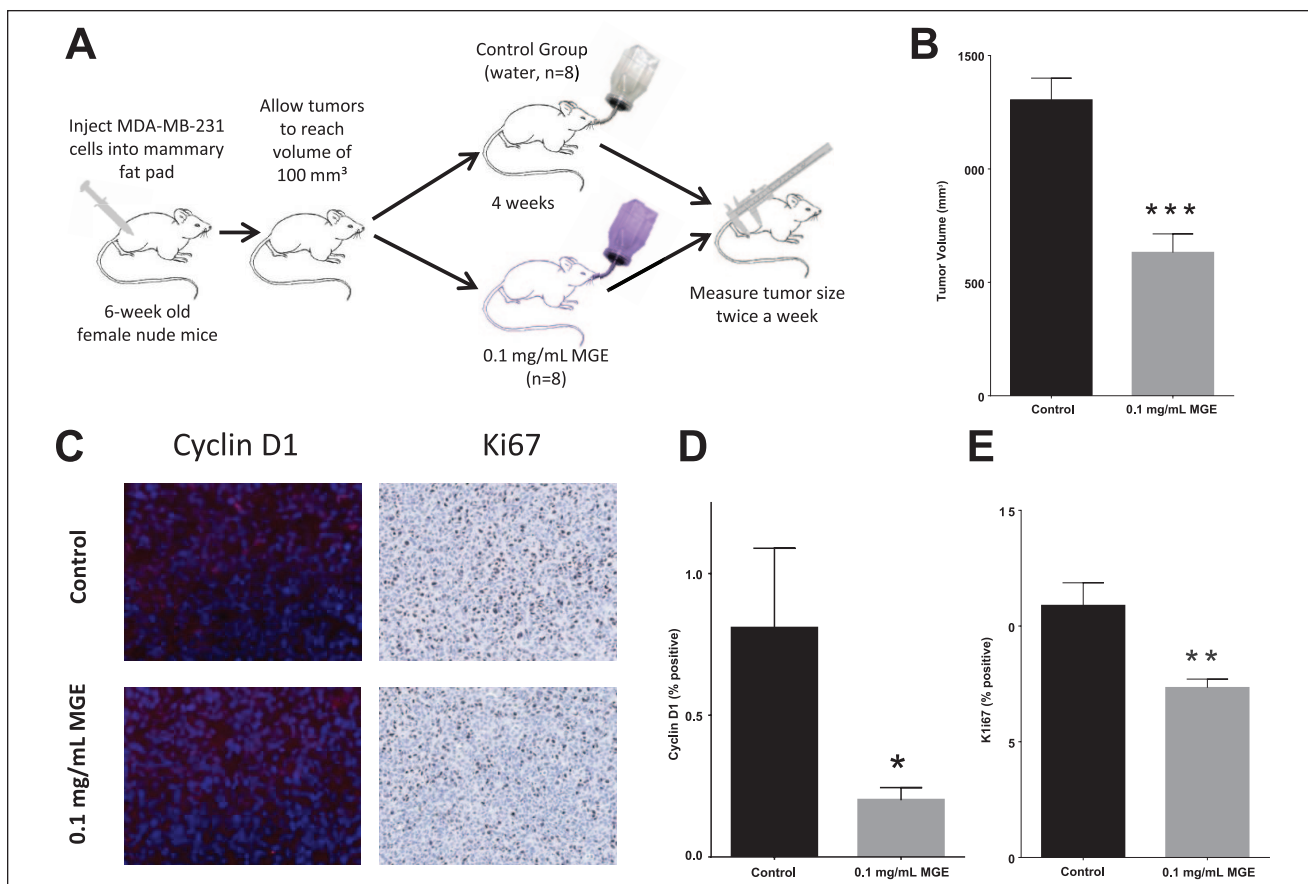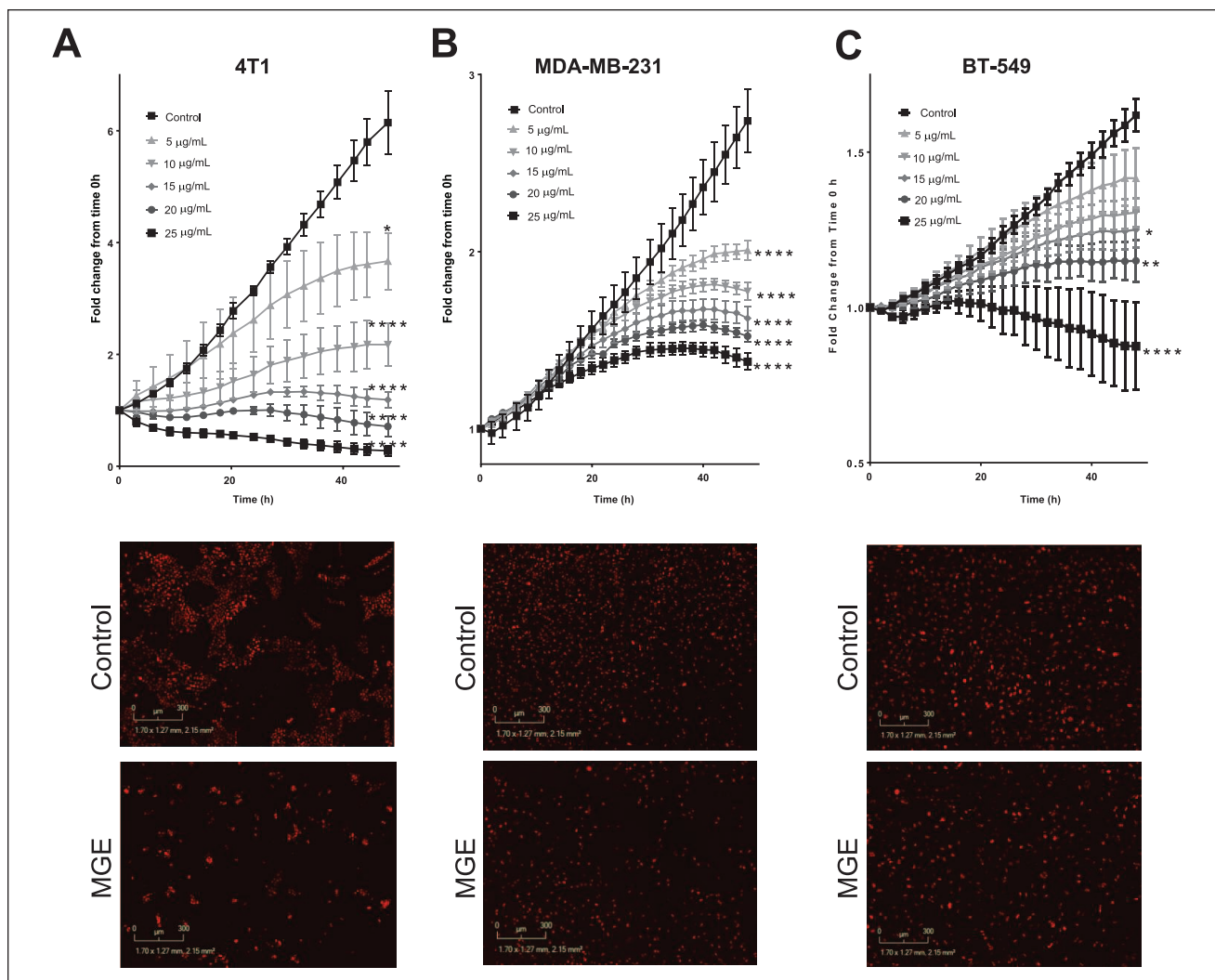
Figure 1. Muscadine grape extract (MGE) inhibits tumor growth *in vivo*. Female nude mice with MDA-MB-231 tumors were treated with 0.1 mg phenolics/mL of MGE for 4 weeks, as shown in the schematic (A). Tumor size was measured at 4 weeks, prior to euthanasia (B). Immunohistological analysis of cyclin D1, which is stained red in the representative images, and Ki67, which is shown as brown with 3,3′-diaminobenzidine (DAB) staining in representative images (C), was quantified (D and E). n = 8; *$P < .05$, **$P < .01$, and ***$P < .001$.

that the extract regulates AKT signaling more effectively in MDA-MB-231 cells.

The effect of MGE on the proliferative ERK/MAPK signaling pathway, another downstream target of c-Met, was also assessed by western blot analysis. MGE (20 µg total phenolics/mL) reduced c-Raf in 4T1 cells by 31.4%, as shown in Figure 4A. MGE at concentrations of both 10 µg total phenolics/mL and 20 µg total phenolics/mL reduced c-Raf in MDA-MB-231 cells by 55.3% and 77.4%, respectively, and in BT-549 cells by 64.9% and 72.4%, respectively (Figure 4B and C). Representative c-Raf western blot bands are depicted below each graph. The reduction in c-Raf total protein could result from a decrease in *RAF1* transcription, the gene encoding c-Raf. *RAF1* mRNA was significantly reduced as early as 6 hours after treatment with MGE in MDA-MB-231 and BT-549 cells (Figure 4E and F). After 24 hours of treatment with 20 µg total phenolics/mL of MGE, *RAF1* mRNA was decreased by 61.8% in MDA-MB-231 cells

and by 44.2% in BT-549 cells. MGE had no effect on *RAF1* expression in 4T1 cells, suggesting that the decrease in c-Raf was not due to changes in *RAF1* expression in this cell line (Figure 4D).

Phosphorylation and activation of MEK and ERK are downstream of c-Raf. Both phospho-MEK and phospho-ERK, normalized to total MEK and ERK, respectively, were reduced in 4T1 and BT-549 cells treated with both 10 µg total phenolics/mL and 20 µg total phenolics/mL of MGE (Figure 5A and C). The higher dose of MGE reduced MEK activation by over 50% and ERK1/2 activation by over 75% in 4T1 cells. However, MGE had no significant effect on MEK or ERK1/2 phosphorylation in MDA-MB-231 cells despite the reduction in c-Raf protein expression (Figure 5B). Representative western blots with phosphorylated MEK or ERK1/2 and respective total proteins are shown for each cell line (Figure 5A-C). These results suggest that MAPK/ERK signaling was differentially regulated by MGE in TNBC cells.

Figure 2. Muscadine grape extract (MGE) inhibits TNBC proliferation. Mouse 4T1 (A), human MDA-MB-231 (B), and human BT-549 (C) TNBC cells labeled with NucLight Red were incubated with increasing concentrations of MGE, and cell proliferation was measured every 2 hours for 48 hours. Cell proliferation was quantified by the number of red nuclei normalized to the number of red nuclei at time 0 hour. Representative images of cells incubated with 20 µg phenolics/mL of MGE for 24 hours are shown in the lower images. n = 3; *$P < .05$, **$P < .01$, and ****$P < .0001$.

Cyclin D1 and Cell Cycle Progression are Reduced in MGE-Treated TNBC Cells

Both AKT and ERK/MAPK signaling pathways positively regulate cyclin D1.[28-32] Cyclin D1 was decreased by 88.0% in 4T1 cells and 88.7% in MDA-MB-231 cells treated with 20 µg total phenolics/mL of MGE (Figure 6A and B). Representative cyclin D1 western blots are shown below the graphs for each cell line, displaying the reduction in cyclin D1 protein with MGE treatment. A time-dependent reduction in the mRNA for *CCND1*, the gene encoding cyclin D1, was observed in both the 4T1 and MDA-MB-231 cell lines following treatment with MGE (Figure 6D and E). Cyclin D1 was not detectable in BT-549 cells (data not

shown). These results suggest that MGE reduces cyclin D1, a protein that contributes to cell cycle progression, through transcriptional regulation of the *CCND1* gene or by destabilization of the *CCND1* transcript in 4T1 and MDA-MB-231 TNBC cells.

Cyclin D1 associates with cyclin-dependent kinase 4/6 (CDK4/6) to regulate retinoblastoma protein (Rb) activation. When cyclin D1 levels are low, CDK4/6 is inactive and cannot phosphorylate Rb to release it from the E2F transcription factor, repressing the transcription of E2F target genes. MGE reduced Rb phosphorylation by over 80% in MDA-MB-231 TNBC cells treated with 10 µg total phenolics/mL or 20 µg total phenolics/mL of MGE, which increases the proportion of E2F-bound,
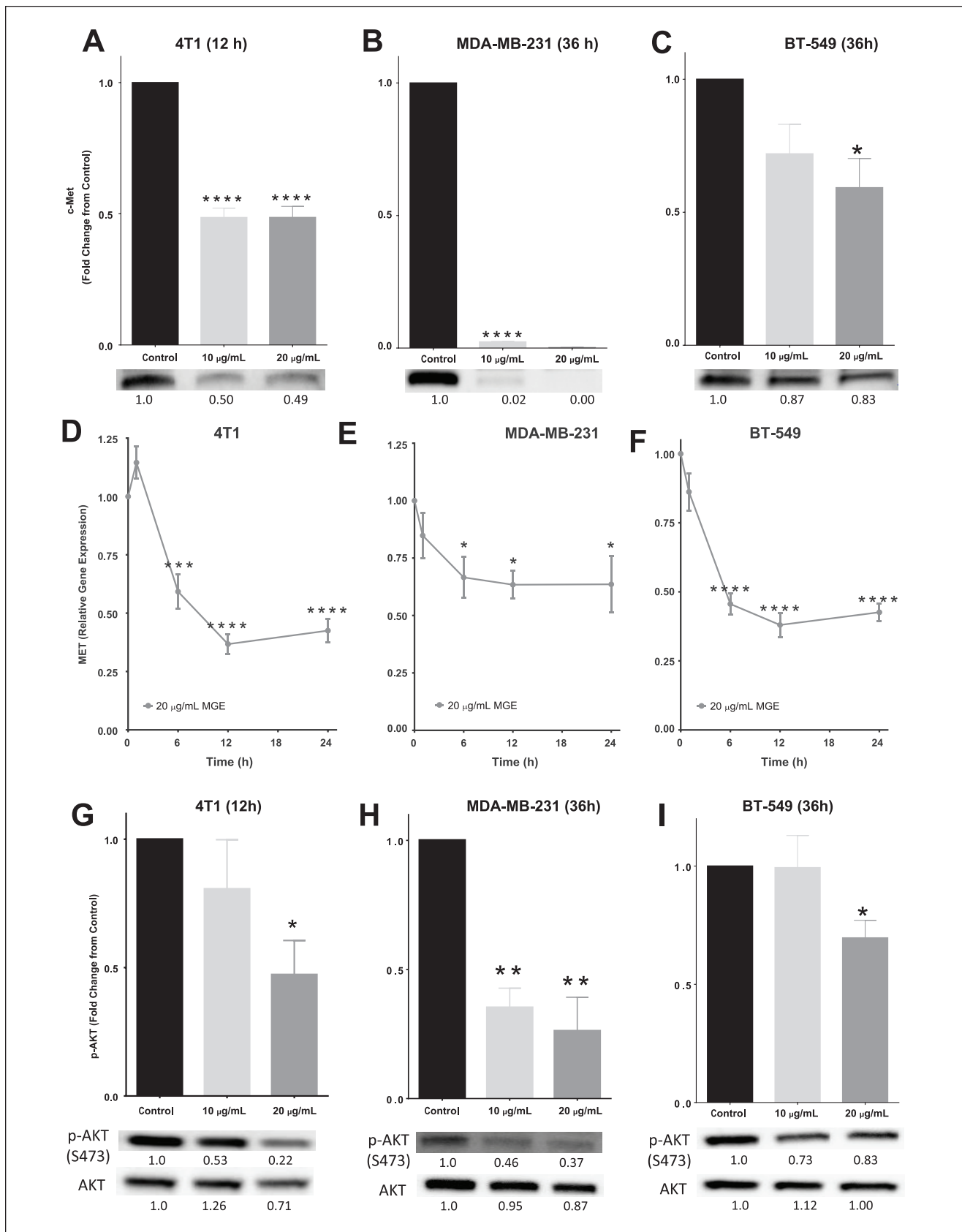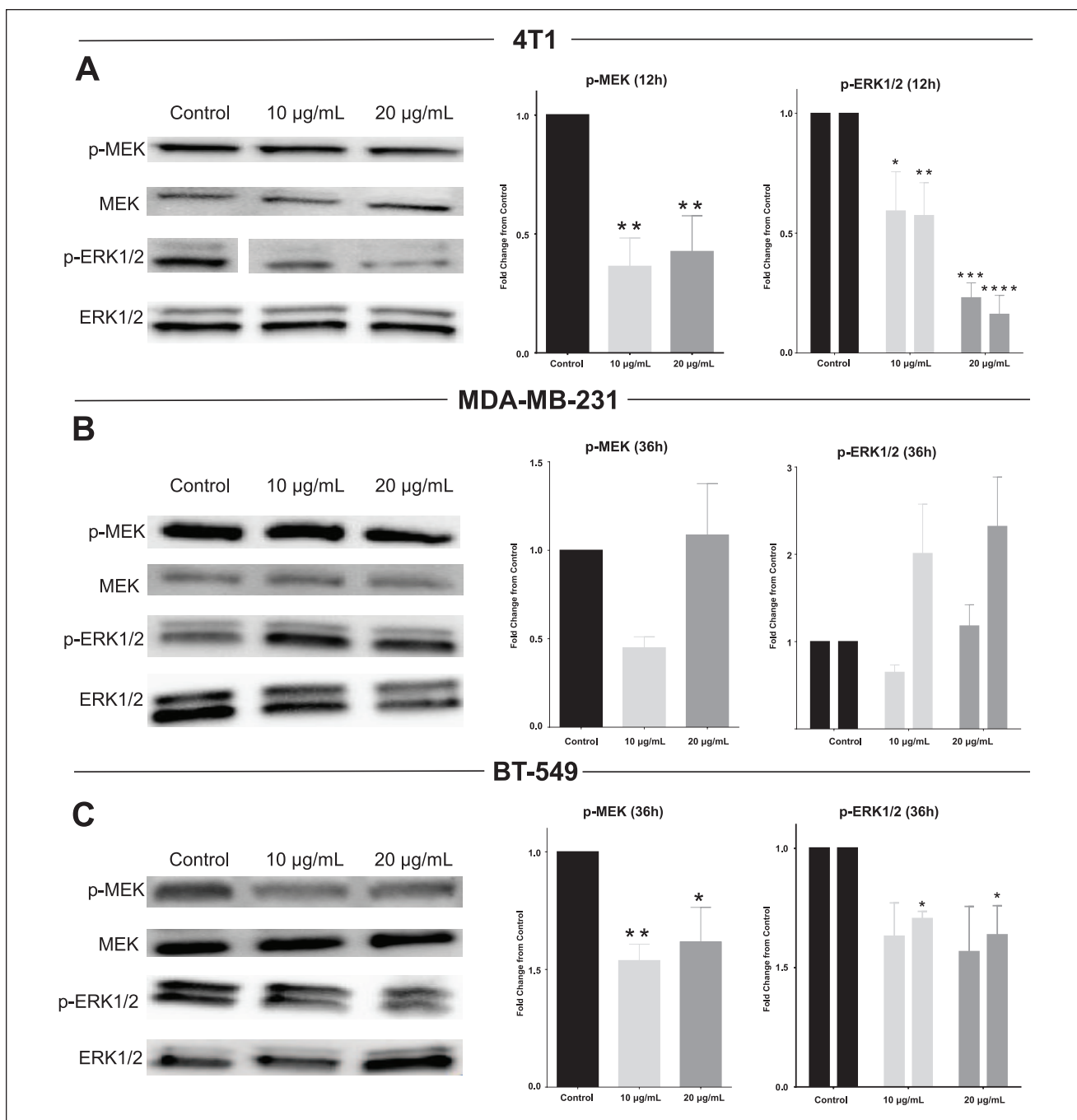
Figure 3. *(continued)*

Figure 3. Muscadine grape extract (MGE) reduces c-MET, *MET*, and AKT activation. 4T1 (A), MDA-MB-231 (B), and BT-549 (C) cells were treated with 10 µg phenolics/mL or 20 µg phenolics/mL of MGE for either 12 or 36 hours, as indicated, and analyzed by western blot. Representative bands are shown below the graphs for each cell type and relative fold-change in band intensity compared with control is shown below the western blot bands. 4T1 (D), MDA-MB-231 (E), and BT-549 cells (F) were treated with 20 µg phenolics/mL of MGE for 1, 6, 12, or 24 hours, and *MET* gene expression was measured by quantitative real-time polymerase chain reaction (qRT-PCR). 4T1 (G), MDA-MB-231 (H), and BT-549 (I) cells were treated with either 10 µg phenolics/mL or 20 µg phenolics/mL of MGE for 12 or 36 hours, and phosphorylation of AKT at Ser473 and total AKT were measured by western blot. p-AKT was normalized to total AKT protein. Representative bands are shown below the graphs for each cell type. Relative fold-change in band intensity compared with the control for both p-AKT and AKT are shown below the western blot bands. n = 3 to 6; *P < .05, **P < .01, ***P < .001, and ****P < .0001.
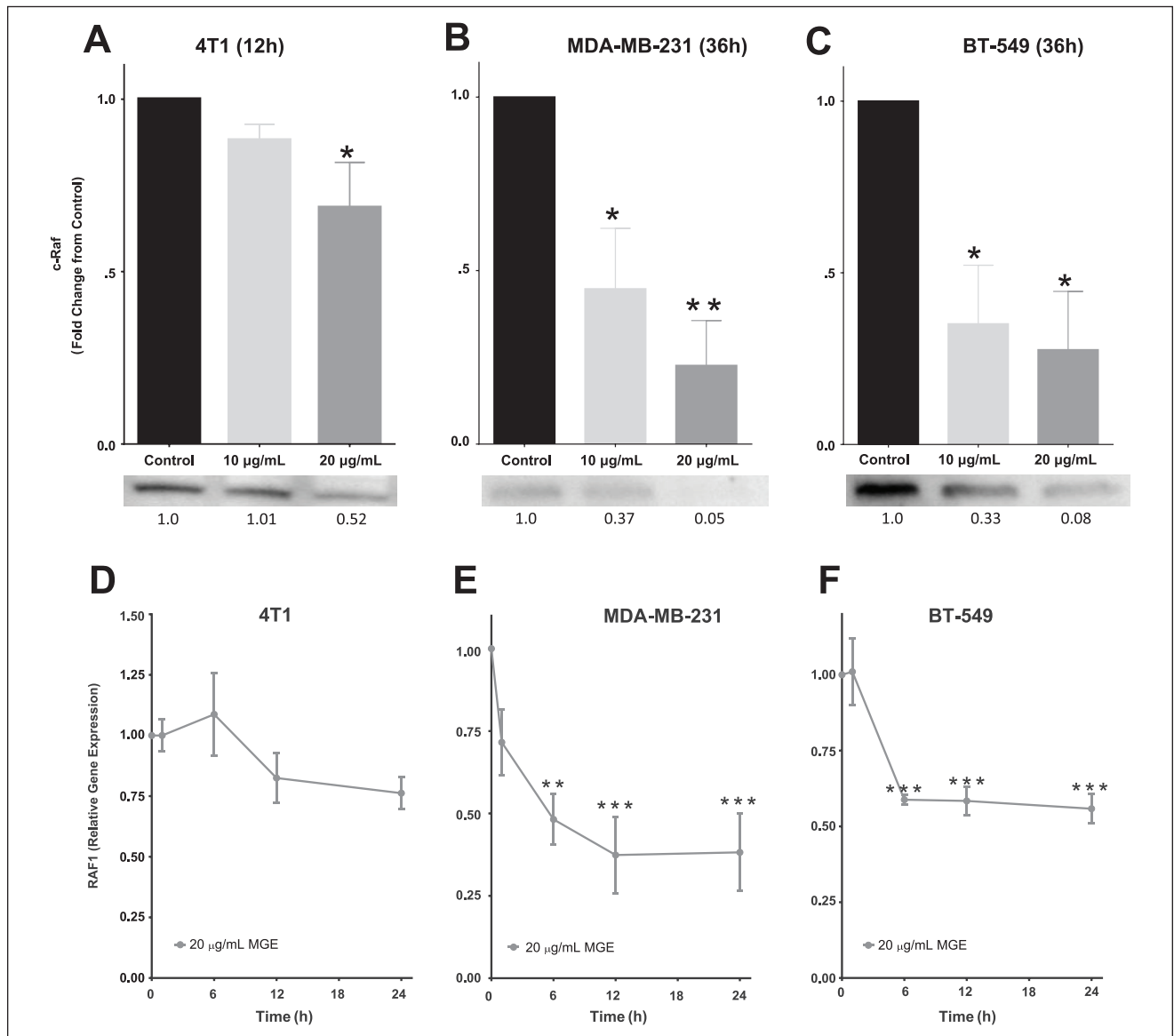
Figure 4. Muscadine grape extract (MGE) inhibits c-Raf and *RAF1*. c-Raf protein was measured by western blot analysis in 4T1 (A), MDA-MB-231 (B), and BT-549 (C) cells treated with 10 µg phenolics/mL or 20 µg phenolics/mL of MGE for either 12 or 36 hours, as indicated. Representative bands are shown below the graphs for each cell type. Relative fold-change in band intensity compared with the control is shown below the western blot bands. 4T1 (D), MDA-MB-231 (E), and BT-549 (F) cells were treated for 1, 6, 12, or 24 hours with 20 µg phenolics/mL of MGE, and *RAF1* was measured by qRT-PCR. n = 3 to 5; *P < .05, **P < .01, and ***P < .001.

Figure 5. Muscadine grape extract (MGE) reduces ERK/MAPK signaling. 4T1 (A), MDA-MB-231 (B), and BT-549 (C) cells were treated for either 12 or 36 hours with 10 μg phenolics/mL or 20 μg phenolics/mL of MGE, and protein lysates were analyzed by western blot. p-MEK was normalized to total MEK, and p-ERK1/2 were normalized separately to ERK1 or ERK2. For bar graphs representing ERK1/2, the first bar in each pair represents p-ERK1/ERK1, and the second bar represents p-ERK2/ERK2. Representative blots are shown to the left of the graphs for each cell line. n = 3 to 5; *$P < .05$, **$P < .01$, ***$P < .001$, and ****$P < .0001$.

active, unphosphorylated Rb protein (Figure 6C). These results suggest that MGE prevents phosphorylation of Rb through attenuated cyclin D1 and thereby may repress E2F targets in TNBC.

Subsequent cell cycle analysis showed that treatment of MDA-MB-231 cells with 20 μg total phenolics/mL of MGE for 24 hours increased the percentage of cells in the G0/G1 phase from $64.8 \pm 1.8\%$ to $71.1 \pm 1.7\%$ ($P < .05$),
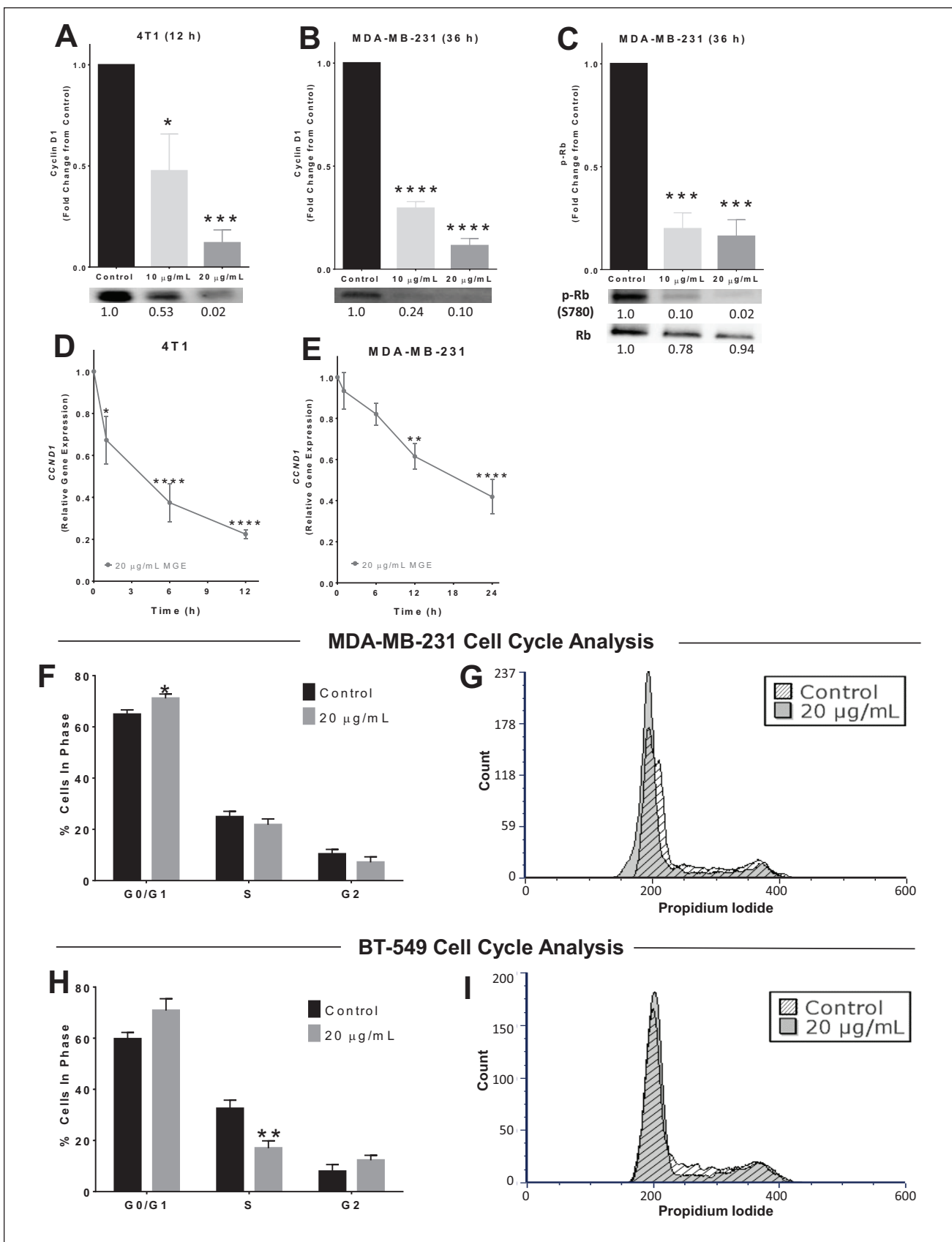
Figure 6. *(continued)*

Figure 6. Muscadine grape extract (MGE) reduces cyclin D1, Rb, and cell cycle progression. 4T1 (A) or MDA-MB-231 (B) cells were treated with either 10 µg phenolics/mL or 20 µg phenolics/mL of MGE for 12 or 36 hours, as indicated, and cyclin D1 was measured by western blot. Representative blots for cyclin D1 protein are shown below the quantitative graphs, and the relative fold-change in band intensity compared with control is shown below western blot bands. 4T1 (D) or MDA-MB-231 (E) cells were treated with 20 µg phenolics/mL of MGE for 1, 6, 12, or 24 hours, and *CCND1*, the gene that encodes cyclin D1, was measured by quantitative real-time polymerase chain reaction (qRT-PCR). (C) MDA-MB-231 cells were treated with 10 µg phenolics/mL or 20 µg phenolics/mL of MGE for 36 hours, and phosphorylation of Rb at S780 (p-Rb) and total Rb protein were measured by western blot. p-Rb was normalized to total Rb protein. Representative bands are shown below the quantitative graph, and the relative fold-change in band intensity compared with the control is shown below the western blot bands. For cell cycle analysis, MDA-MB-231 (F and G) and BT-549 (H and I) cells were treated with 20 µg phenolics/mL of MGE for 24 hours. The bar graphs indicate the percentage of cells in each phase of the cell cycle for untreated control cells compared with MGE-treated cells (F and H). Histograms of representative samples show the amount of propidium iodide staining within cells on the *x*-axis and the number of cells on the *y*-axis (count), with the peak at 200 indicating G0/G1 phase, the peak at 400 indicating G2 phase, and cells with levels of propidium iodide in between the peaks representative of S phase (G and I). Histograms of control (diagonal lines) and MGE-treated (shaded) cells were overlaid and normalized by total cell count. n = 3 to 5; $*P < .05$, $**P < .01$, $***P < .001$, and $****P < .0001$.

indicating that the extract causes G0/G1 cell cycle arrest in this cell line (Figure 6F). In BT-549 cells, treatment with 20 µg total phenolics/mL of MGE for 24 hours reduced the amount of cells in S phase by 47.7% ($P < .05$), suggesting that cells may be accumulating in the G0/G1 or G2 phase (Figure 6H). Representative histograms show the relative amount of cells in each phase of the cell cycle after 24 hours with or without MGE treatment (Figure 6G and I). Treatment with MGE for 24 hours did not cause significant changes in 4T1 cell cycle progression (data not shown). These results show that the effect of MGE on cell cycle progression is different in each of the TNBC cell lines, suggesting that the extract exhibits diverse antiproliferative mechanisms between TNBC cell lines.

Discussion

Muscadine grape extract reduced TNBC tumor size and tumor cyclin D1 and Ki67 in mice, demonstrating that MGE reduces breast tumor growth *in vivo* in association with effects on proliferation. MGE also reduced c-Met and differentially suppressed signaling of downstream AKT and ERK/MAPK pathways in TNBC cells *in vitro*, as diagrammed in Supplemental Figure 2 (available online). This reduction was associated with inhibition of the cyclin D1/Rb/E2F axis, differential effects on cell cycle progression, and an ultimate decrease in TNBC cell proliferation.

c-Met protein overexpression is recognized as a poor prognostic factor for invasive breast cancers, and its importance in TNBC led to several phase II clinical trials that examined the effect of c-Met inhibitors in combination with other drugs on TNBC.[33] The reduction in c-Met and *MET* mRNA by MGE in 4T1 and BT-549 TNBC cells suggests that the extract reduces c-Met transcription; however, the more pronounced reduction in c-Met protein in MDA-MB-231 cells indicates that additional mechanisms may be involved besides transcription of *MEt al*one. MGE may alter c-Met endosomal recycling or lysosomal degradation, which occurs after c-Met activation by phosphorylation to end c-Met signaling.[34] MGE may also

increase c-Met ubiquitin-mediated protein degradation in MDA-MB-231 cells to lead to the enhanced reduction in c-Met.

In addition to c-Met, MGE may affect other receptor tyrosine kinases that also regulate downstream AKT and ERK/MAPK signaling, such as the EGFR and vascular endothelial growth factor receptor (VEGFR).[35] EGFR and VEGFR are often overexpressed in TNBC.[23,36] Inhibition of either of these receptors or a reduction in their expression could contribute to MGE's inhibitory effects on AKT and ERK/MAPK signaling. Although MGE reduced AKT and/or ERK/MAPK signaling in all TNBC cell lines, the effects were different in each cell line. MGE did not inhibit MAPK/ERK signaling in MDA-MB-231 cells. MDA-MB-231 TNBC cells have a gain of function mutation in KRAS and BRAF, which leads to constitutive activation of MAPK signaling[37]; treatment with MGE may not be able to overcome the enhanced ERK/MAPK signaling in these cells. In contrast, MGE reduced AKT signaling in all 3 of the TNBC cell lines studied. However, the extract was the least effective at inhibiting AKT phosphorylation in BT-549 cells, which harbor a loss of function PTEN mutation, leading to enhanced activation of the AKT pathway.[37] Nevertheless, MGE significantly reduced both MEK and ERK signaling in BT-549 cells. In contrast to BT-549 and MDA-MB-231 cells, 4T1 TNBC cells harbor no mutations in either the ERK/MAPK or AKT signaling pathways, and MGE markedly inhibited both of these signaling pathways in the 4T1 cells. These disparate results demonstrate the heterogeneous nature of TNBC, which is why it is essential to study the effect of therapeutics in multiple TNBC cell lines that have distinct mutations.[38]

Although MGE differentially abrogated the ERK/MAPK and AKT signaling pathways in the 3 TNBC cell lines examined, MGE reduced cyclin D1 mRNA and protein in both 4T1 and MDA-MB-231 cells. This could be due to either ERK/MAPK or AKT inhibition since both signaling pathways can regulate cyclin D1 transcription and expression by numerous mechanisms. Reduced AKT activation

can cause cyclin D1 degradation by ubiquitination through GSK3β.[39] Alternatively, AKT and ERK can signal through mTORC1 to activate eukaryotic initiation factor 4E (eIF4E) and promote cap-dependent translation of *CCND1*.[19,40] Both ERK and AKT can also promote *CCND1* transcription via negative regulation of FOXO3a, a transcription factor with tumor suppressive effects.[41,42] ERK can also promote *CCND1* transcription via TOB and AP-1 transcription factors, which are involved in cell proliferation control.[32,43] Due to the complexity of cyclin D1 regulation by AKT and ERK signaling pathways and the diverse bioactive components present in the MGE preparation, MGE likely controls cyclin D1 by several AKT- and/or ERK-regulated mechanisms in TNBC cells.

As expected with reduced cyclin D1 expression, MGE caused G0/G1 cell cycle arrest in MDA-MB-231 cells.[29] However, the effect was modest and likely does not exclusively account for the reduction in MDA-MB-231 proliferation by MGE. Furthermore, no changes in cell cycle progression were observed in 4T1 cells with MGE treatment despite the reduction in cyclin D1, suggesting that alternate mechanisms are contributing to reduced cell proliferation. Since MGE did not cause apoptosis, the extract could promote necrotic or autophagic cell death[44]; both AKT and ERK/MAPK are involved in autophagy through mTOR signaling.[45] Although autophagy or necrosis could also contribute to the MGE-reduced proliferation in BT-549 cells, these cells showed marked changes in cell cycle kinetics. BT-549 cells contain a low cyclin D1 concentration compared with other breast cancer cell lines and do not contain RB1, suggesting that MGE does not inhibit proliferation of BT-549 cells through an attenuated cyclin D1/Rb/E2F axis.[46,47] However, transcription factors regulated by AKT and ERK/MAPK such as FOXO3a and AP-1 can reduce proliferation through mechanisms distinct from cyclin D1 regulation. For example, FOXO3a transcription factors can upregulate p21^{Cip1} or p27^{KIP1}, which are cyclin-dependent kinase inhibitors, to inhibit cell cycle progression.[48] Upregulation of either of these inhibitors could lead to accumulation of cells in G0/G1 or G2 phase, which could explain the reduction of MGE-treated BT-549 cells in S phase compared with untreated cells.

Muscadine grape extract significantly reduced proliferation in all 3 TNBC cell lines examined, even though there are differences in the molecular mechanisms affected by MGE in the 3 cell lines, likely due in part to unique mutations in MAPK, AKT, and Rb signaling. This is important because significant heterogeneity exists within TNBC, which contributes to the difficulty in developing successful therapies for this aggressive breast cancer subtype.[23] In spite of the heterogeneity between these 3 TNBC cell lines, MGE inhibited proliferation in each cell line, likely due to different mechanisms of action by the multiple compounds present in the MGE preparation.

Many drugs tested in clinical trials for the treatment of TNBC targeted 1 specific molecular pathway and failed due to acquired or inherent cancer cell resistance.[21] Because of the developed resistance, the paradigm for developing adjuvant treatments for TNBC is shifting toward combination therapies; however, significant hurdles to combinatorial therapies exist. In particular, combination therapies often increase the development of side effects relative to each single agent drug alone, due to the side effects observed with the individual components.[38] Natural products in their unfractionated states have the potential to affect multiple cellular targets, as shown in this study, with few side effects. Thus, MGE is a naturally occurring combination therapy. In fact, the preparation of MGE used in these studies upregulated or downregulated hundreds of different pathways in TNBC cells in a genome-wide microarray analysis (unpublished data).

Currently, an ongoing Phase 1 clinical trial at the Wake Forest Comprehensive Cancer Center is assessing the safety and tolerability of the MGE formulation examined in this study in patients with advanced solid tumors (NCT02583269).[49] Patients are treated for 4 weeks at 5 doses of MGE, from 320 to 1600 mg total phenolics/day (or the equivalent of 5 to 24 mg/kg/day for a 70 kg man). The extract was well tolerated, to date, with no adverse events greater than grade 3, and a maximal tolerated dose has not yet been reached. At a dose within the same range administered to patients in our Phase 1 clinical study, we showed that MGE significantly reduced TNBC tumor growth in mice with daily administration of 0.5 mg total phenolics/day, which equates to 20 mg total phenolics/kg/day. The safety and tolerability of treating patients with a different MGE preparation isolated from muscadine grape skins was previously observed in a multi-institutional trial in men with recurrent prostate cancer[8]; no adverse side effects other than grade 1 gastrointestinal symptoms were reported and no dose-limiting toxicities were observed in this trial. These results suggest that effective doses of our proprietary MGE will be safe to use since it is well tolerated in patients at a dose that was effective in preclinical studies of triple-negative breast tumors in mice. Thus, the extract may be useful for the treatment of TNBC.

Conclusion

Triple-negative breast cancer patients currently have no therapeutic options once initial standard of care is complete, despite the relatively high likelihood of developing metastasis within 5 years of diagnosis. Approximately 20% of cancer patients currently use plant-derived products as a complementary and alternative treatment for the prevention of cancer recurrence and metastasis, a percentage that has consistently risen within the past couple of decades.[50] Our results demonstrated that the MGE used in

our preclinical and clinical studies appears to be safe and well-tolerated; MGE effectively reduced tumor growth in mice and inhibited oncogenic signaling in TNBC cells. This suggests that the extract may be an effective nutraceutical as an adjuvant to standard of care to treat women with TNBC.

Author Contributions

MC, EAT, and PEG designed the research, wrote the article, and had oversight. MC conducted research, analyzed data, and had primary responsibility for final content. All authors read and approved the final manuscript.

Declaration of Conflicting Interests

The author(s) declared no potential conflicts of interest with respect to the research, authorship, and/or publication of this article.

ORCID iD

E. Ann Tallant (iD) https://orcid.org/0000-0003-4162-4373

Supplemental Material

Supplemental material for this article is available online.

References

1. Breastcancer.org. Breast cancer statistics. https://www.breast-cancer.org/symptoms/understand_bc/statistics. Published 2017. Accessed April 6, 2020.
2. Lund MJ, Butler EN, Hair BY, et al. Age/race differences in HER2 testing and in incidence rates for breast cancer triple subtypes: a population-based study and first report. *Cancer*. 2010;116:2549-2559.
3. Badve S, Dabbs DJ, Schnitt SJ, et al. Basal-like and triple-negative breast cancers: a critical review with an emphasis on the implications for pathologists and oncologists. *Mod Pathol*. 2011;24:157-167.
4. Dent R, Hanna WM, Trudeau M, Rawlinson E, Sun P, Narod SA. Pattern of metastatic spread in triple-negative breast cancer. *Breast Cancer ResTreat*. 2009;115:423-428.
5. Anders CK, Carey LA. Biology, metastatic patterns, and treatment of patients with triple-negative breast cancer. *Clin Breast Cancer*. 2009;9(suppl 2):S73-S81.
6. Weinberg RA. *The Biology of Cancer*. 2nd ed. New York, NY: Garland Science; 2013.
7. Ullah MF, Bhat SH, Husain E, et al. Cancer chemopreventive pharmacology of phytochemicals derived from plants of dietary and non-dietary origin: implication for alternative and complementary approaches. *Phytochem Rev*. 2014;13:811-833.
8. Paller CJ, Rudek MA, Zhou XC, et al. A phase I study of muscadine grape skin extract in men with biochemically recurrent prostate cancer: safety, tolerability, and dose determination. *Prostate*. 2015;75:1518-1525.
9. You Q, Chen F, Sharp JL, Wang X, You Y, Zhang C. High-performance liquid chromatography–mass spectrometry and evaporative light-scattering detector to compare phenolic profiles of muscadine grapes. *J Chromatogr A*. 2012;1240:96-103.
10. Liu KC, Huang AC, Wu PP, et al. Gallic acid suppresses the migration and invasion of PC-3 human prostate cancer cells via inhibition of matrix metalloproteinase-2 and -9 signaling pathways. *Oncol Rep*. 2011;26:177-184.
11. Moon JH, Eo SK, Lee JH, Park SY. Quercetin-induced autophagy flux enhances TRAIL-mediated tumor cell death. *Oncol Rep*. 2015;34:375-381.
12. Jeong MH, Ko H, Jeon H, et al. Delphinidin induces apoptosis via cleaved HDAC3-mediated p53 acetylation and oligomerization in prostate cancer cells. *Oncotarget*. 2016;7:56767-56780.
13. Wang L, Li W, Lin M, et al. Luteolin, ellagic acid and punicic acid are natural products that inhibit prostate cancer metastasis. *Carcinogenesis*. 2014;35:2321-2330.
14. Mertens-Talcott SU, Lee JH, Percival SS, Talcott ST. Induction of cell death in Caco-2 human colon carcinoma cells by ellagic acid rich fractions from muscadine grapes (*Vitis rotundifolia*). *J Agric Food Chem*. 2006;54:5336-5343.
15. Hudson TS, Hartle DK, Hursting SD, et al. Inhibition of prostate cancer growth by muscadine grape skin extract and resveratrol through distinct mechanisms. *Cancer Res*. 2007;67:8396-8405.
16. Luo JM, Song SR, Wei Z, Huang Y, Zhang YL, Lu J. The comparative study among different fractions of muscadine grape "Noble" pomace extracts regarding anti-oxidative activities, cell cycle arrest and apoptosis in breast cancer. *Food Nutr Res*. 2017;61:1412795.
17. Ignacio DN, Mason KD, Hackett-Morton EC, et al. Muscadine grape skin extract inhibits prostate cancer cells by inducing cell-cycle arrest, and decreasing migration through heat shock protein 40. *Heliyon*. 2019;5:e01128.
18. Cancer Genome Atlas Network. Comprehensive molecular portraits of human breast tumours. *Nature*. 2012;490:61-70.

19. Vivanco I, Sawyers CL. The phosphatidylinositol 3-kinase AKT pathway in human cancer. *Nat Rev Cancer*. 2002;2:489-501.

20. Wu WS, Hu CT. *Signal Transduction in Cancer Metastasis*. Dordrecht, Netherlands: Springer; 2010.

21. Jin X, Mu P. Targeting breast cancer metastasis. *Breast Cancer (Auckl)*. 2015;9(suppl 1):23-34.

22. Giltnane JM, Balko JM. Rationale for targeting the Ras/MAPK pathway in triple-negative breast cancer. *Discov Med*. 2014;17:275-283.

23. Oualla K, El-Zawahry HM, Arun B, et al. Novel therapeutic strategies in the treatment of triple-negative breast cancer. *Ther Adv Med Oncol*. 2017;9:493-511.

24. Lee A, Djamgoz MBA. Triple negative breast cancer: emerging therapeutic modalities and novel combination therapies. *Cancer Treat Rev*. 2018;62:110-122.

25. Duncan AV, Pirro NT, Tallant A, Gallagher PE, Chappell MC. A Targeted UHPLC-MS approach to quantify phenolics in muscadine grape supplements. *FASEB J*. 2017;31(1 suppl):646.1.

26. Rivero-Gutiérrez B, Anzola A, Martínez-Augustin O, de Medina FS. Stain-free detection as loading control alternative to Ponceau and housekeeping protein immunodetection in western blotting. *Anal Biochem*. 2014;467:1-3.

27. Organ SL, Tsao MS. An overview of the c-MET signaling pathway. *Ther Adv Med Oncol*. 2011;3(1 suppl):S7-S19.

28. Mendoza MC, Er EE, Blenis J. The Ras-ERK and PI3K-mTOR pathways: cross-talk and compensation. *Trends Biochem Sci*. 2011;36:320-328.

29. Alao JP. The regulation of cyclin D1 degradation: roles in cancer development and the potential for therapeutic invention. *Mol Cancer*. 2007;6:24.

30. Jirmanova L, Afanassieff M, Gobert-Gosse S, Markossian S, Savatier P. Differential contributions of ERK and PI3-kinase to the regulation of cyclin D1 expression and to the control of the G1/S transition in mouse embryonic stem cells. *Oncogene*. 2002;21:5515-5528.

31. Klein EA, Assoian RK. Transcriptional regulation of the cyclin D1 gene at a glance. *J Cell Sci*. 2008;121(pt 23):3853-3857.

32. Shaulian E, Karin M. AP-1 in cell proliferation and survival. *Oncogene*. 2001;20:2390-2400.

33. Ho-Yen CM, Jones JL, Kermorgant S. The clinical and functional significance of c-Met in breast cancer: a review. *Breast Cancer Res*. 2015;17:52.

34. Peters S, Adjei AA. MET: a promising anticancer therapeutic target. *Nat Rev Clin Oncol*. 2012;9:314-326.

35. Butti R, Das S, Gunasekaran VP, Yadav AS, Kumar D, Kundu GC. Receptor tyrosine kinases (RTKs) in breast cancer: sig-naling, therapeutic implications and challenges. *Mol Cancer*. 2018;17:34.

36. Ueno NT, Zhang D. Targeting EGFR in triple negative breast cancer. *J Cancer*. 2011;2:324-328.

37. American Type Culture Collection. *ATCC® Cell Lines by Gene Mutation*. Manassas, VA: American Type Culture Collection; 2014.

38. Bianchini G, Balko JM, Mayer IA, Sanders ME, Gianni L. Triple-negative breast cancer: challenges and opportunities of a heterogeneous disease. *Nat Rev Clin Oncol*. 2016;13:674-690.

39. Takahashi-Yanaga F, Sasaguri T. GSK-3beta regulates cyclin D1 expression: a new target for chemotherapy. *Cell Signal*. 2008;20:581-589.

40. Averous J, Fonseca BD, Proud CG. Regulation of cyclin D1 expression by mTORC1 signaling requires eukaryotic initiation factor 4E-binding protein 1. *Oncogene*. 2008;27:1106-1113.

41. Schmidt M, de Mattos SF, van der Horst A, et al. Cell cycle inhibition by FoxO forkhead transcription factors involves down-regulation of cyclin D. *Mol Cell Biol*. 2002;22:7842-7852.

42. Liu Y, Ao X, Ding W, et al. Critical role of FOXO3a in carcinogenesis. *Mol Cancer*. 2018;17:104.

43. Suzuki T, K-Tsuzuku J, Ajima R, Nakamura T, Yoshida Y, Yamamoto T. Phosphorylation of three regulatory serines of Tob by Erk1 and Erk2 is required for Ras-mediated cell proliferation and transformation. *Genes Dev*. 2002;16:1356-1370.

44. Green DR, Llambi F. Cell death signaling. *Cold Spring Harb Perspect Biol*. 2015;7:a006080.

45. Golden EB, Pellicciotta I, Demaria S, Barcellos-Hoff MH, Formenti SC. The convergence of radiation and immunogenic cell death signaling pathways. *Front Oncol*. 2012;2:88.

46. Bartkova J, Lukas J, Muller H, Lützhøft D, Strauss M, Bartek J. Cyclin D1 protein expression and function in human breast cancer. *Int J Cancer*. 1994;57:353-361.

47. Robinson TJW, Liu JC, Vizeacoumar F, et al. RB1 status in triple negative breast cancer cells dictates response to radiation treatment and selective therapeutic drugs. *PLoS One*. 2013;8:e78641.

48. Zhang X, Tang N, Hadden TJ, Rishi AK. Akt, FoxO and regulation of apoptosis. *Biochim Biophys Acta*. 2011;1813:1978-1986.

49. Bitting RL, Tooze JA, Petty WJ, et al. Phase I study of muscadine grape extract in advanced malignancy. *J Clin Oncol*. 2018;36(15 suppl):e14548. doi:10.1200/JCO.2018.36.15_suppl.e14548

50. Watkins CL, Fernandez-Robles C, Miller KM, Pine A, Stern TA. Use of complementary and alternative medicine by patients with cancer. *Prim Care Companion CNS Disord*. 2011;13:PCC.10f01011.